Retroviral Gene Therapy Vectors for Prevention of Excimer Laser–Induced Corneal Haze

Ashley Behrens,[1,2] *Erlinda M. Gordon,*[3,4] *Li Li,*[2] *Peng X. Liu,*[3] *Zhenhai Chen,*[3] *Hongjun Peng,*[3] *Laurie La Bree,*[5] *W. French Anderson,*[3,4,6] *Frederick L. Hall,*[3,7] *and Peter J. McDonnell*[1,2]

Purpose. To determine the in vivo efficacy and safety of a retroviral vector bearing an antiproliferative dominant negative mutant cyclin G1 (dnG1) construct, when used for the prevention of corneal haze after phototherapeutic keratectomy (PTK).

Methods. For in vivo efficacy studies, a 6-mm-diameter, 150-μm-deep transepithelial PTK, performed with a clinical 193-nm ArF excimer laser (VISX Star2, Santa Clara, CA) was performed on the left eyes of 20 adult New Zealand White rabbits. The surgically altered eyes were subsequently treated with eye drops containing: a retroviral vector bearing a dnG1 construct (dnG1; $n = 7$), a control retroviral vector (null vector) bearing only the neomycin resistance, *neo*^{r}, gene ($n = 7$), or a retroviral vector bearing an antisense cyclin G1 (aG1) construct ($n = 6$). The time of closure of the corneal epithelial defect was monitored daily with fluorescein staining. Corneal haze was evaluated before surgery and at 2, 3, and 4 weeks after surgery, with a digital imaging system. Biodistribution studies for detection of potential vector dissemination to nontarget organs were conducted by PCR-based assay.

Results. The re-epithelialization rate was similar among treatment groups, with complete closure of the corneal epithelial defect at 72 hours ($P > 0.05$). Significant corneal haze developed in the null and aG1 vector–treated groups ($P \leq 0.05$) at 3 to 4 weeks after PTK. In contrast, development of corneal haze was inhibited in the dnG1 vector–treated group when compared with the null vector-treated group ($P < 0.05$). In parallel, a dramatic reduction to complete abrogation of abnormal extracellular matrix production was noted in the dnG1 vector–treated corneas when compared with the null and aG1 vector–treated groups. Biodistribution studies showed no evidence of vector dissemination in neighboring and distant organs.

Conclusions. At therapeutic doses, eye drop application of the dnG1 retroviral vector is safe and effective in inhibiting development of corneal haze after PTK in rabbits. (*Invest Ophthalmol Vis Sci.* 2002;43:968–977)

From the [1]Department of Ophthalmology, Doheny Eye Institute and the [3]Gene Therapy Laboratories and the Departments of [4]Pediatrics, [7]Surgery, [5]Preventive Medicine, and [6]Biochemistry, University of Southern California School of Medicine, Los Angeles, California; and the [2]Department of Ophthalmology, University of California Irvine, Irvine, California.

Supported by the James Gipson Foundation, Los Angeles, California.

Submitted for publication May 29, 2001; revised October 25, 2001; accepted November 30, 2001.

Commercial relationships policy: N.

The publication costs of this article were defrayed in part by page charge payment. This article must therefore be marked "*advertisement*" in accordance with 18 U.S.C. §1734 solely to indicate this fact.

Corresponding author: Peter J. McDonnell, Department of Ophthalmology, University of California Irvine, 118 Med Surg I, Irvine, CA 92697; pjmcdonn@uci.edu.

Variable degrees of corneal haze with the subsequent loss of best corrected visual acuity is a common complication of superficial laser keratectomy. In 3% of patients who undergo minimal to moderately high-level correction and in up to 15% of patients who undergo high-level correction for myopia, the laser-induced corneal haze is enough to impair visual acuity.[1] The pathophysiologic events after laser application on corneal tissue in animal models have been extensively studied. Normally, the anterior stroma of the cornea is hypocellular, and only a few keratocytes (corneal fibroblasts) are found within abundant type I collagen.[2,3] Shortly after laser surgery, these cells begin to incorporate DNA precursors,[4] undergo transformation into activated fibroblasts, rapidly proliferate, and migrate to the area of laser injury, resulting in a hypercellular anterior stromal compartment.[2,5,6] These activated keratocytes synthesize new collagen and extracellular matrices that distort normal corneal architecture.[7,8] Further, activated keratocytes are able to transdifferentiate into myofibroblasts, which can cause contraction of the cornea.[9] These wound-healing responses act in concert to induce corneal opacification and, consequently, regression of the intended refraction. Other investigators believe that corneal haze is caused primarily by the high numbers of bright reflecting keratocytes present in the anterior stromal compartment of the cornea.[10]

Based on these observations, therapeutic reduction of keratocyte proliferation after laser surgery may abrogate the triggering of a cascade of events involved in development of corneal haze, thereby preventing its occurrence. Previous studies have demonstrated the efficacy of retroviral vectors bearing cell cycle modulators in inhibiting keratocyte proliferation in vitro,[11] and of concentrated vectors bearing the herpes simplex virus thymidine kinase (HSV-tk) gene followed by ganciclovir in preventing development of corneal haze in vivo.[12–14] However, the use of HSV-tk vectors has been associated with tissue necrosis,[15] thus preventing its use for inhibition of corneal haze in humans. The purpose of the present study was to evaluate the in vivo efficacy and safety of antiproliferative retroviral vectors bearing modified cell cyclin G1 constructs for prevention of development of corneal haze after excimer laser phototherapeutic keratectomy (PTK).

Methods

Construction of the Dominant Negative Cyclin G1 Construct in the Retroviral Expression Vector

Figure 1A–D shows the pdnG1/pREX cyclin G1 retroviral vector plasmid containing the deletion mutant of the human cyclin G1 gene,[16,17] encoding amino acids 41 to 249 transcribed from the cytomegalovirus (CMV) promoter. The vector also contains retroviral packaging sequences and the bacterial neomycin phosphotransferase (*neo*^{r}) gene transcribed from an internal simian virus (SV)40 early promoter. The truncated cyclin G1 gene was initially cloned into the pG1XsvNa vector (provided by Genetic Therapy, Inc., Gaithersburg, MD) which contains a Psi sequence. The pREX expression vector was created by inserting the *Kpn*I fragment of pG1(dnG1)SvNa into *Kpn*I digested

Investigative Ophthalmology & Visual Science, April 2002, Vol. 43, No. 4

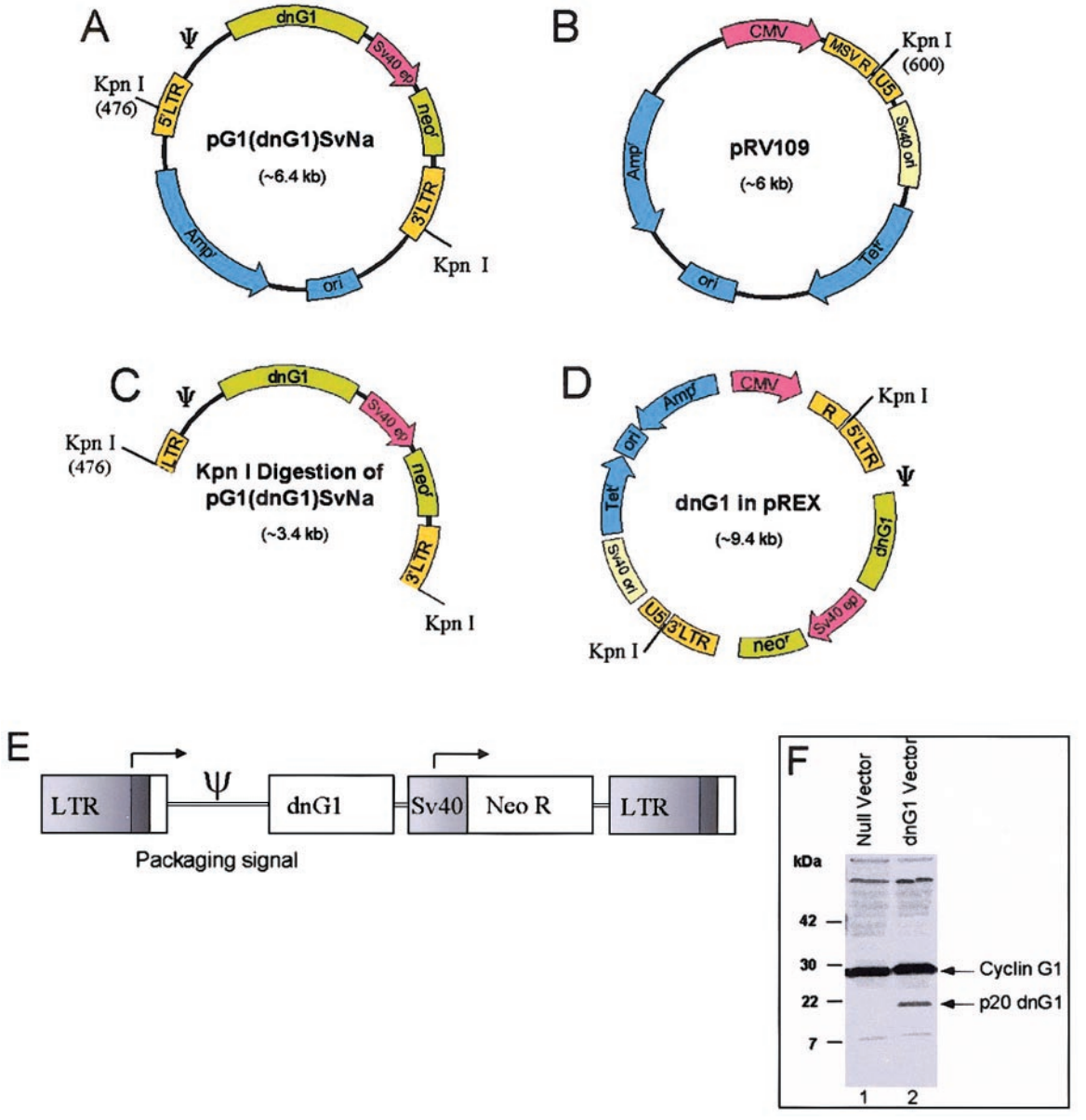

FIGURE 1. Synthesis of the (dnG1) construct in the retroviral expression vector (pREX). (**A**) The MLV-based pdnG1/pREX cyclin G1 retroviral vector plasmid containing the deletion mutant of the human cyclin G1 gene (dnG1) encoding amino acids 41 to 249 transcribed from the CMV promoter and the bacterial neomycin phosphotransferase, *Neo*^{r}, gene transcribed from an internal SV40 early promoter were used. The truncated cyclin G1 gene was initially cloned into the pG1XsvNa vector. (**B**) The *Kpn*I fragment of pG1(dnG1)SvNa was inserted into (**C**) the *Kpn*I-digested pRV109. (**D**) The resultant pREX expression vector containing a hybrid CMV-MSV LTR sequence and the mutant cyclin G1. (**E**) A simplified diagram of the dnG1 retroviral vector, wherein the N-terminal deletion mutant construct was cloned initially into a TA cloning vector, followed by *Not*I-*Sal*I digestion and ligation of the purified insert into a *Not*I–*Sal*I digested pG1XSvNa retroviral expression vector to produce the pdnG1SvNa vector complete with 5′ and 3′ LTR sequences and psi retroviral packaging sequence. (**F**) Western analysis of lysates from dnG1-transduced HT29 cells. A distinct immunoreactive band in the region of 20 kDa indicates expression of the mutant dnG1 protein while the endogenous cyclin G1 protein is seen as an intensely staining band in the region of ~30 kDa. The expression of the dnG1 protein in transduced cells results in unscheduled cell death; hence, the low level expression of the dnG1 protein in cell lysates from transduced unselected cell cultures.

pRV109 (provided by Alan Kingsman, University of Oxford, Oxford, UK). The resultant pREX plasmid contains a hybrid CMV/MSV LTR sequence. A simplified diagram of the dominant negative cyclin G1 (dnG1) retroviral vector is depicted in Figure 1E.

Cells, Cell Culture Conditions, and Plasmid Expression Vectors Bearing Marker Genes

NIH3T3 and 293T cells were supplied by the American Type Culture Collection (Manassas, VA). NIH 3T3 and 293T cells were maintained in Dulbecco's modified Eagle's medium (DMEM) supplemented with 10% fetal bovine serum (FBS; D10; BioWhittaker, Walkersville, MD). The plasmids pcgp containing the viral *gag pol* genes, and a retroviral vector, pcnBg, expressing a nucleus-targeted β-galactosidase construct were kindly provided by Paula Cannon and Ling Li, respectively (University of Southern California Gene Therapy Laboratories, Los Angeles, CA).

Retroviral Vector Production

High-titer vectors were generated using a transient three-plasmid co-transfection system,[18] in which the packaging components *gag-pol*, a

wild-type murine leukemia virus-based amphotropic CAE envelope (*env*), or a chimeric *env* bearing a von Willebrand factor (vWF)–derived collagen-binding (matrix targeting) motif and a retroviral vector bearing either a nucleus-targeted β-galactosidase gene or a dnG1 construct expressed from the CMV promoter were placed on separate plasmids, each of which contained the SV40 origin of replication. For comparisons of in vivo efficacy, a nontargeted retroviral vector bearing an antisense cyclin G1 construct (aG1)[19–22] and a nontargeted retroviral vector bearing only the *neo*^{r} gene (null control) were used.

Viral Titers

Viral titers were determined in murine NIH3T3 cells, as described previously, based on expression of the β-galactosidase or *neo*^{r} gene.[19] Viral titer was expressed as the number of β-galactosidase–expressing colonies or G418-resistant colony-forming units (CFU) per milliliter. For the in vivo marker study, the titer of both the targeted and nontargeted nBg vector was 1×10^7 CFU/mL. For the in vivo efficacy studies, the titer of each vector (dnG1, null or aG1) was approximately 5×10^7 CFU/mL. For vector safety studies, three increasing doses of the dnG1 vector (dose level I, 5×10^6 CFU/mL; dose level II, 5×10^7 CFU/mL; dose level III, 1×10^8 CFU/mL) were used.

Assay for Biological Activity (Inhibitory Activity) of the dnG1 Retroviral Vector

A standard assay for inhibitory activity in transduced target CT26 cells was conducted as previously described.[19] The cells were cultured as monolayers at a plating density of 1×10^5 cells per well, in D10. After overnight attachment, the cells were exposed to 1 mL of the dnG1 vector or to medium alone as the control in the presence of a transfection reagent (8 μg/mL; Polybrene; Sigma Chemical Co., St. Louis, MO) for 2 hours, with periodic rocking. Then, 1 mL D10 was added to each well, and the cultures were further incubated at 37°C in a 5% CO_2 incubator. The medium was replaced with 2 mL fresh D10 the next day. To assess the inhibitory activity of the dnG1 vector, the transduced cells were evaluated for their proliferative potential by counting the number of viable cells in triplicate cultures at serial intervals (0, 24, 48, and 72 hours) after transduction without G418 selection. For verification of biological activity, a progressive decrease in cell number was noted in dnG1 vector–treated cultures, whereas the medium-treated cultures showed a progressive increase in cell number.[23] The mean cell number in the dnG1 vector–treated cultures at 48 hours was then compared with that of control cultures and expressed as a percentage of inhibitory activity. Using this assay, the inhibitory activity of the dnG1 vector used for the in vivo efficacy studies was 74%.

Western Blot Analysis for Expression of the dnG1 Protein in Transduced Target Cells

Verification of mutant dnG1 protein expression in transduced G418 unselected HT29 target cells was conducted. A distinct immunoreactive dnG1 in the region of 20 kDa indicated expression of the mutant dnG1 protein, whereas the endogenous cyclin G1 protein was seen as an intensely staining band in the region of ~30 kDa (Fig. 1F). The expression of the dnG1 protein in transduced cells resulted in unscheduled cell death—thus, the low-level expression of the dnG1 protein in cell lysates from transduced unselected cell cultures.[23]

Experimental Animals for Retroviral Transduction of Cornea by Ophthalmic Drops

After approval by the Institutional Animal Care and Use Committee of the University of Southern California and according to the guidelines of the ARVO Statement for the Use of Animals in Ophthalmic and Vision Research, 30 adult New Zealand White rabbits were included in the study. The mean weight of the animals on arrival was 8.5 ± 0.89 lb (SD). The rabbits were examined at the slit lamp after 2 days in the vivarium, to rule out presence of external ocular disease, such as discharge, conjunctival injection, or corneal scarring. To evaluate the efficiency of gene delivery to laser-treated cornea by eye drop application, four rabbits were treated with either a targeted or nontargeted vector bearing a marker gene. To evaluate the efficacy of the antiproliferative constructs, 20 rabbits were randomly labeled 1 to 20, and assigned to receive either a control or a therapeutic vector (treatment scheme described later). Four additional rabbits were treated with increasing concentrations of the dnG1 vector to evaluate retroviral toxicity and vector dissemination to nontarget organs.

Excimer Laser PTK

In rabbits under general anesthesia (ketamine and xylazine), a lid speculum was inserted in the left eye of each, 2 to 4 drops of tetracaine 0.5% (Alcaine; Alcon, Fort Worth, TX) were instilled topically, and a transepithelial PTK 6-mm in diameter and 150 μm in depth was performed. A clinical 193-nm excimer laser (Star2; Visx Inc., Santa Clara, CA) with parameters set at 160-mJ/cm^2 fluence, 20-ns pulse, and 8-Hz repetition rate was used. During the laser ablation, the treated area was exposed to a nitrogen gas blower to maximize the development of corneal haze after surgery, as previously reported.[24]

Treatment Scheme for Retroviral Vector Transduction

One hour after the surgery, instillation of eye drops of the solution containing a vector was initiated. Investigators performing instillation were masked for the treatment applied. The vials were labeled with letters A, B, and C, according to the vector administered. The topical application sequence was similar to the numeric values assigned to the rabbits: vector A to rabbit 1, vector B to rabbit 2, vector C to rabbit 3, and so forth. Each rabbit received one 40-μL eye drop of vector every 10 minutes for a 2-hour period on the first day, and the same scheme for 1.5 hours on the second day. Rabbits in the vector A group received a collagen-targeted retroviral vector bearing a dnG1 construct ($n = 7$); the vector B group received a retroviral null vector bearing only the *neo*^{r} gene ($n = 7$), and the vector C group received a retroviral vector bearing an aG1 construct ($n = 6$). The cumulative vector dose for each rabbit in all three groups was approximately 5×10^7 CFU.

Vector Efficacy Studies

Corneal haze monitoring was conducted by an observer who was blinded to the type of vector treatment. Objective corneal haze assessment was performed using a tangential slit lamp (Model BL900; Haag-Streit, Köniz, Switzerland) focused on the surface of the cornea and oriented at a 45° angle of incidence to this plane. The image reflected was recorded by digital photography (DCTRV-8; Sony Corp., Tokyo, Japan) at a 90° angle to the corneal surface. Lighting conditions in the room and in the slit lamp source were controlled to be similar to avoid bias at the time of the image analysis. Images were downloaded into a computer by means of a digital image capture software (Studio DV 1.05.303; Pinnacle Systems Inc., Mountain View, CA) at a 1500 × 1125-pixel resolution and evaluated by a digital imaging analysis software (Image 4.0.2; Scion Corp., Frederick, MD). For corneal haze assessment, a modified procedure of objective corneal haze measurement was used.[13,25] For calibration and standardization to enable comparisons between rabbits, each image was transformed into gray-scale and three areas of 50 × 50 pixels each were measured within the light reflection (superior, middle, and inferior). The imaging software recognizes different shades of gray in a scale from 1 (white) to 255 (black). According to the different tones within the selected area, a mean shade number of gray is assigned. The lower the units obtained, the higher the corneal haze (Fig. 2). Standardization of the procedure was performed by using an initial measurement of the nonablated cornea as baseline. The software assigns a number to this baseline value from which the numbers from succeeding measurements at different time points are adjusted. This standardization procedure reduces the possibility of measurement errors arising from the variable lighting conditions. For evaluation of transduction efficiency, the harvested corneas of β-galactosidase vector–treated rabbits were quick

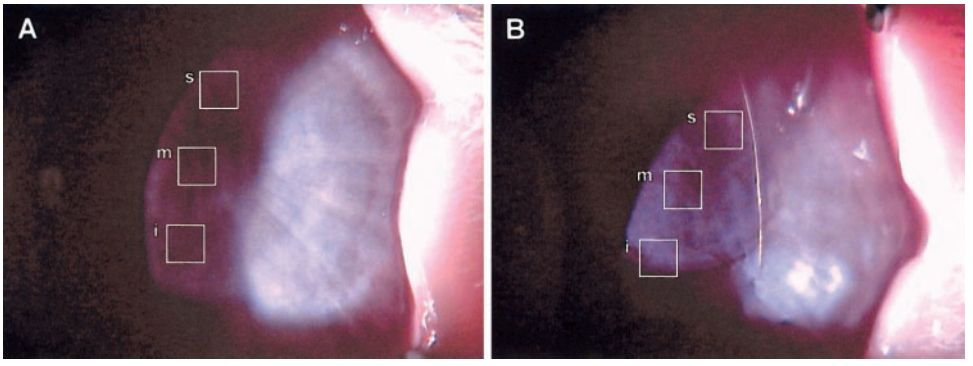

FIGURE 2. Selection of the areas for corneal haze measurement. (**A**) Postoperative low-degree corneal haze after 4 weeks of observation. The mean scores in the three measured areas (s, superior; m, middle; and i, inferior) was 179.4. (**B**) Moderate-degree of corneal haze after 4 weeks of observation. The mean score in the three areas was 161.1.

frozen in liquid nitrogen and stained with X-Gal histochemical stain for presence of β-galactosidase activity.[23] Immunohistochemistry studies for detection of abnormal extracellular matrix production was performed in tissue sections of harvested corneas from the vector-treated groups using a mouse anti-cellular fibronectin monoclonal antibody (MAB1940; Chemicon International, Inc., Temecula, CA), with species reactivities to human, rat, rabbit, or guinea pig fibronectin.

Safety Study 1: Evaluation of Corneal Re-epithelialization. Evaluation of re-epithelialization and corneal haze were performed by the same observer in a masked fashion. Epithelial defect closure was monitored daily. After topical instillation of fluorescein drops (Fluorostrip, Haag-Streit), a digital photograph (DCTRV-8) under slit lamp with cobalt blue light (Portable Slit Lamp; Carl Zeiss, Oberkochen, Germany) was recorded. For the re-epithelialization assessment, the epithelial defect area stained with fluorescein was measured after previous calibration to a known scale value included in the photograph frame. Rabbits were killed at day 28 after the surgery, and both eyes were subjected to histologic analysis. Both right and left eyes were enucleated and immersed in buffered paraformaldehyde 10% for 24 hours. The eyes were bisected at the central area of the keratectomy and embedded in paraffin. Thin sections (5 μm) were stained with hematoxylin-eosin in each specimen slide.

Safety Study 2: Vector Toxicity and Biodistribution. After determining the vector group most efficient in corneal haze prevention, an additional group of six rabbits (three female, three male) were subjected to studies of toxicity with three increasing dosages of the dnG1 vector. One male rabbit and one female rabbit were selected for each dosage group. The same PTK and eye drop application scheme was used. A modified Draize score was used to gauge external toxicity.[26] This group of animals were killed at 2 weeks, and histologic evaluation of paraformaldehyde-fixed tissue sections with PAS staining, was conducted to rule out signs of ocular inflammation.

Tissue samples of target and nontarget organs were also obtained for biodistribution studies. For these studies, specimens were frozen in liquid nitrogen. The ocular adnexa (eyelids), nasal mucosa, nasal septum, and contralateral eye were evaluated for evidence of vector dissemination to nontarget organs. Further, vital organs such as brain, heart, lung, liver, spleen, kidney, testis, and ovary were harvested for biodistribution studies.

Vector Biodistribution Analysis

A quantitative PCR analysis for the presence of vector DNA sequences was performed (Althea Technologies, San Diego, CA). The dnG1 vector is an amphotropic retroviral vector derived from the G1XSvNa vector (Genetic Therapy, Inc.) which was fused with the RV109 vector, as described previously.[17,18] A PCR assay (*Taq*Man; PE-Applied Biosystems, Foster City, CA) was developed to detect the G1XSvNa-based vector containing SV40 and neomycin (*Neo*) gene sequences into mouse genomic DNA background. The assay detects a 95-nucleotide (nt) amplicon (nts 1779–1874 of the G1XSvNa plasmid vector) in which the fluorescently labeled probe overlaps the 3′ portion of the SV40 gene and the 5′ portion of the *Neo* gene. The lower limit of detection for the assay is 10 copies of G1XSvNa plasmid vector. The lower limit of quantitation is 100 copies of G1XSvNa plasmid vector.

The precision of the assay was established using mouse DNA samples spiked with G1XSvNa plasmid over six experimental runs. A high degree of intra-assay reproducibility was demonstrated in the standards. The interassay precision was estimated by comparing the means of each sample from the different runs and determining the percentage of covariation. The sensitivity and suitability of the assay when using rabbit tissue samples was determined by spiking the G1XSvNa plasmid standards into the negative sample DNA from each sample extraction set. The spiked samples were run as one to three duplicates. The results of the spiked samples were in close agreement with the standard curve.

Histopathologic Examination of Nontarget Organs

Tissue sections were stained with hematoxylin-eosin stain. Under light microscopy, tissue sections from nontarget organs were evaluated for integrity of organ architecture, detection of cellular swelling or necrosis, presence of acute or chronic inflammation, hypo- or hypercellularity, thrombosis, or any other abnormality.

Statistical Analysis

Numerical data were analyzed by computer (SPSS 10.0 for Windows; SPSS Inc., Chicago, IL). Data describing the epithelial defect area and corneal haze are expressed as the mean ± SD. Comparisons were performed using the paired *t*-test for within-group differences and the analysis of variance for intergroup differences. The Mann-Whitney and Kruskal-Wallis tests were used for histologic keratocyte count comparisons. $P \leq 0.05$ was considered statistically significant.

RESULTS

Retroviral Gene Delivery to Laser-Treated Corneas

After laser surgery, four rabbits received eye drop applications of either a nontargeted (designated CAE-nBg) or a collagen-targeted (designated Mx-nBg) vector bearing a β-galactosidase gene. The cumulative vector dose for each rabbit in both groups was approximately 1×10^7 CFU administered over 2 days. Topographic examination of the laser-injured corneas showed an apparent increase in the number of transduced cells in corneas that were treated with the collagen-targeted vector ($n = 2$) when compared with corneas that received the nontargeted vector ($n = 2$), as evidenced by a fourfold increase in the number of β-galactosidase–expressing cells (Fig. 3, blue dots). There was no β-galactosidase–positive staining noted in the conjunctiva or in the corneal endothelium. Based on this

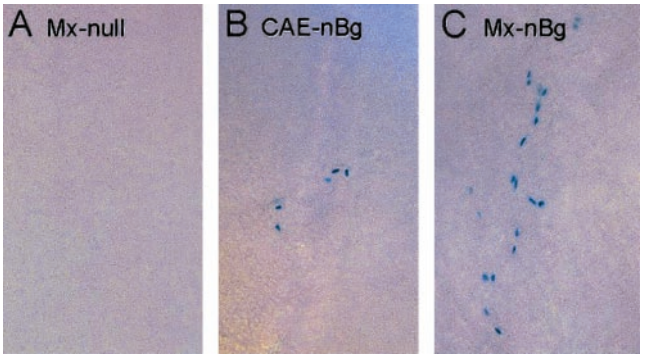

FIGURE 3. Improved retroviral gene delivery to laser-treated corneas is dependent on the vWF's targeting motif displayed on the retroviral *env* protein. After laser surgery, four rabbits received eye drop applications of (**A**) a null vector, (**B**) a nontargeted (designated CAE-nBg) , or (**C**) a collagen-targeted (designated Mx-nBg) vector bearing a β-galactosidase gene. The cumulative vector dose for each rabbit in both groups was approximately 1×10^7 CFU administered over 2 days. Enhanced transduction of the laser-injured corneas ($n = 2$) was noted, with the collagen-targeted vector compared with the nontargeted vector ($n = 2$), as evidenced by a fourfold increase in the number of β-galactosidase–expressing cells (*blue dots*). Based on this finding as well as on previous reports,[23,27–29] a collagen-targeted vector bearing a dnG1 construct was used for the in vivo efficacy studies.

finding as well as on previous reports,[13,23,27–29] a collagen-targeted vector bearing a dnG1 construct was used for the in vivo efficacy studies.

Inhibition of Development of Corneal Haze after Laser Surgery in dnG1 Vector–Treated Eyes

After laser surgery, each rabbit received a topical cumulative vector dose of $\sim 5 \times 10^7$ CFU as eye drops. On evaluation 2 weeks after laser treatment (12 days after vector application), transient changes in corneal transparency were noted in all three groups. However, resolution of corneal opacification was noted after weeks 3 and 4 in the dnG1 vector–treated rabbits (group A), as indicated by objective corneal haze assessment scores (Table 1). In contrast, rabbits treated with the control null vector (group B) and the aG1 vector (group C) showed sustained and progressive development of corneal haze throughout the entire observation period, which was statistically significant by multiple-comparisons *t*-test (Fig. 4; Table 1). Photographs of rabbit eyes showing varying degrees of corneal haze in vector-treated eyes compared with preoperative control eyes by slit lamp examination are shown in Figure 5.

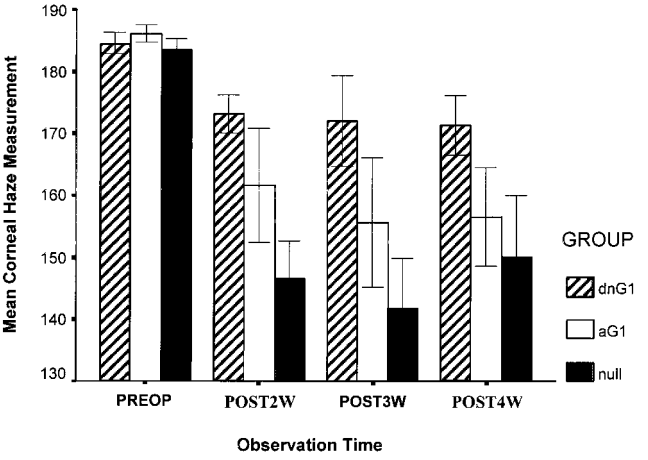

FIGURE 4. Mean preoperative data (PREOP) and mean postoperative data after 2 weeks (POST2W), 3 weeks (POST3W), and 4 weeks (POST4W).

Evaluation of Corneal Re-epithelialization after Laser Surgery

The epithelial defects from all vector-treated corneas were completely closed 4 days after PTK (Fig. 6). No statistical differences were noted in the epithelial defect area between groups analyzed at each postoperative day (Table 2). Similarly, no persistent epithelial defects or ulceration was observed in any of the vector-treated groups, indicating the safety of retroviral vector administration. In terms of local ocular toxicity, no significant differences were noted in the modified Draize score numbers between groups that received increasing doses of the dnG1 vector. Further, the overall score of each dose was considerably low (range fluctuation from 1 to 3, of a maximum toxicity score of 40; Table 3).

TABLE 1. Inhibition of Corneal Haze Development in Laser-Injured Rabbit Eyes by Ophthalmic Instillation of a Retroviral Vector Bearing a Dominant Negative Cyclin G1 Construct

		Postoperative		
	Preoperative	**2 Weeks**	**3 Weeks**	**4 Weeks**
Group A (dnG1)	184.36 ± 4.87	173.11 ± 9.16	171.98 ± 21.89	171.07 ± 14.37
Change from day 0		−11.26 ± 12.41	−12.38 ± 25.30	−13.29 ± 16.55
*P**		0.05	0.24	0.08
Group B (null)	183.57 ± 4.80	146.62 ± 16.66	141.86 ± 22.32	146.05 ± 29.49
Change from day 0		−36.95 ± 18.28	−41.71 ± 22.29	−37.52 ± 31.14
*P**		0.004	0.006	0.03
Group C (aG1)	186.16 ± 3.71	161.53 ± 25.29	155.63 ± 28.55	152.84 ± 27.08
Change from day 0		−24.62 ± 24.15	−30.53 ± 27.01	−33.32 ± 26.76
*P**		0.05	0.04	0.03
ANOVA *P*†	0.60	0.05	0.11	0.77
Pair-wise comparisons	NS	A > B $P \leq 0.05$	NS	NS

Data are the mean ± SD of corneal haze scores.

* Paired *t*-test looking at the within-group change.

† ANOVA *P* for the overall differences between the three groups. If the ANOVA $P \leq 0.05$, then pair-wise comparisons were tested using multiple-comparison *t*-tests, which adjusts the α levels based on the number of pair-wise comparisons that were made.

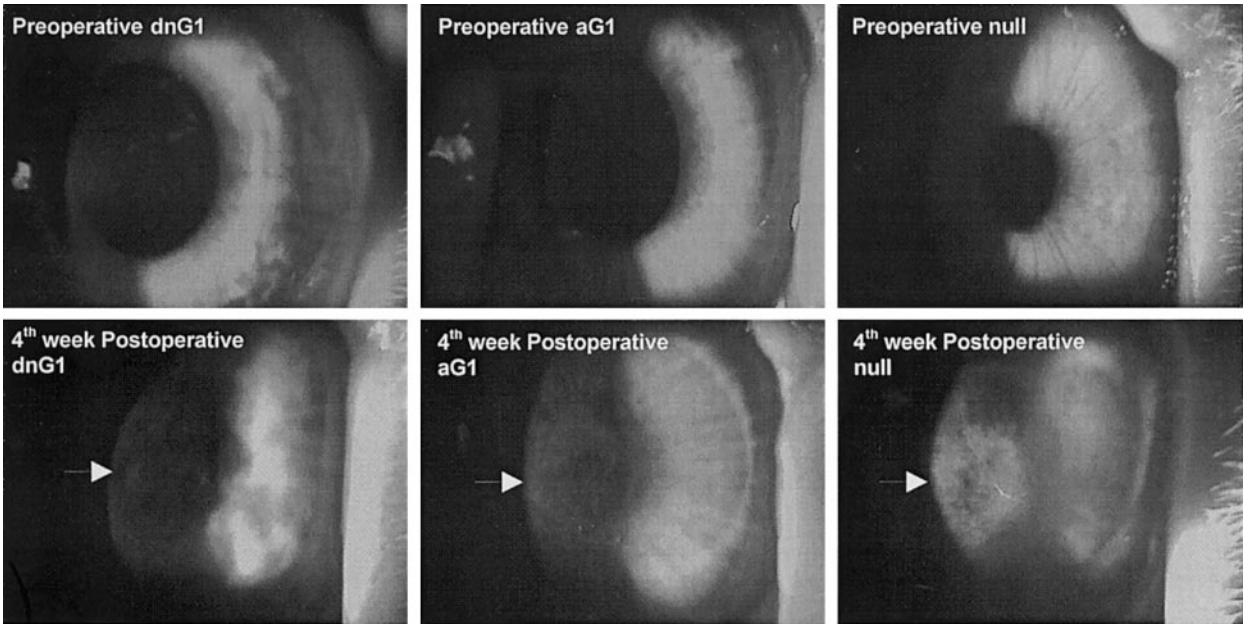

FIGURE 5. Comparison of development of corneal haze: preoperative status (*top*) and 4 weeks after PTK with retroviral vector instillation (*bottom*). The dnG1 group showed less corneal haze (*arrows*) than the aG1 and null control groups.

Normal Rate of Re-epithelialization and Absence of Corneal Defects and Ulcerations in dnG1 Vector–Treated Rabbit Corneas

Seventy-two hours after PTK, complete closure of the corneal epithelial defect was noted in all three groups (Table 2). Histologic examination of paraformaldehyde-fixed tissue sections showed that the epithelial cell layer was intact in all three vector-treated groups, with preservation of cellular polarity, phenotype, and total layer thickness. A significant reduction in superficial keratocyte counts (50 μm of anterior stroma) was observed in the central corneal area at the laser keratectomy site in dnG1 vector–treated corneas compared with control- and aG1 vector–treated corneas (Fig. 7). In the central area of the ablation, at $\times$40 magnification, the mean keratocyte counts were 58 $\pm$ 19.71 (SD), 71 $\pm$ 16.70, and 97.6 $\pm$ 7.79 in the dnG1, aG1, and null vector–treated groups, respectively (P = 0.01). Pair-wise comparisons confirmed significant differences between the dnG1 and null vector–treated groups (P = 0.01) and between the aG1 and null vector–treated groups (P = 0.04). Although the number of keratocytes was less in the dnG1-treated corneas than in the aG1-treated corneas, the difference was not statistically different (P = 0.19). In parallel, the inhibition of keratocyte proliferation was associated with a dramatic reduction to complete abrogation of abnormal extracellular matrix production in the dnG1 vector–treated corneas when compared with the null and aG1 vector–treated groups (Fig. 8). Further, the inner corneal endothelial cell layer showed normal morphology and cell number in all vector-treated groups. One rabbit that received a control null vector and one that received a dnG1 vector showed development of acute bacterial keratitis on the second day after surgery, which necessitated euthanasia.

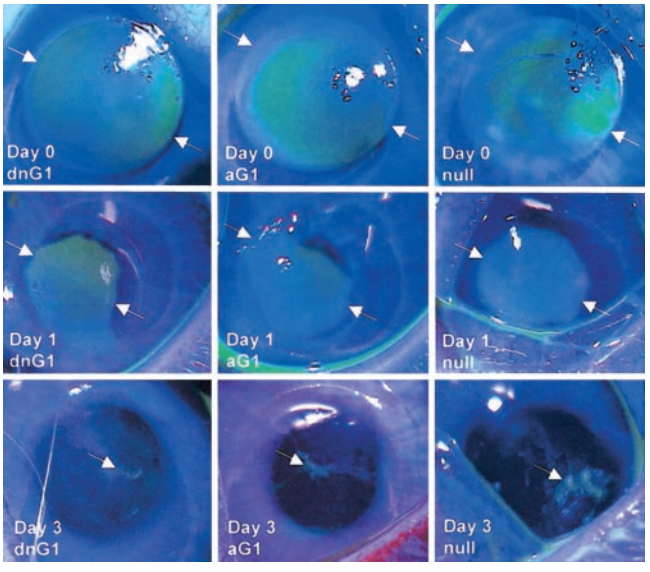

FIGURE 6. The three groups showed similar epithelial defect areas (*between arrows*) at day 0 (*top*), day 1 (*middle*), and day 3 (*bottom*), revealing an intact re-epithelialization process. At day 3, most of the corneas in both groups showed complete epithelial defect closure.

Vector Biodistribution Studies

No evidence of vector dissemination was observed in the upper eyelid, nasal mucosa, nasal septum, and contralateral eye nor in vital organs such as brain, lung, heart, liver, spleen, kidney, testis, and ovary in rabbits that received a dose equivalent to twice the dose planned for the clinical trial. No PCR signal was detected in the left lower eyelid of two animals that received the lowest dose: dose level I (cumulative vector dose, 5×10^6 CFU/eye). Very low level PCR signals were detected in the left lower eyelids of two of two animals that received dose level II (10 and 24 copies/μg DNA; cumulative vector dose, 5.7×10^7 CFU/eye), and in one of two animals that received dose level III (26 copies/μg DNA; cumulative vector dose, 1×10^8 CFU/eye), which is equivalent to twice the highest dose planned for the clinical trial. These positive signals were below the limits of quantification but were slightly over the limits of detection, as determined by the *Taq* PCR assay. The clinical significance of this low-level PCR signal is presently unclear.

TABLE 2. Re-epithelialization of Laser-Injured Rabbit Eyes after Ophthalmic Instillation of a Retroviral Vector Bearing a Dominant Negative Cyclin G1 Construct

	Day 0	24 Hours	48 Hours	72 Hours
Group A (dnG1)	30.80 ± 0.76	16.29 ± 4.16	1.39 ± 0.86	0.14 ± 0.21
Change from day 0		−14.51 ± 4.64	−29.41 ± 1.39	−30.66 ± 0.86
*P**		0.0002	0.0001	0.0001
Group B (null)	29.49 ± 0.44	14.53 ± 2.55	1.54 ± 1.20	0.19 ± 0.37
Change from day 0		−14.96 ± 2.15	−27.95 ± 0.90	−29.30 ± 0.63
*P**		0.0001	0.0001	0.0001
Group C (aG1)	29.77 ± 1.99	16.79 ± 2.98	2.37 ± 1.83	0.20 ± 0.28
Change from day 0		−12.98 ± 3.07	−27.40 ± 2.27	−29.57 ± 1.97
*P**		0.0001	0.0001	0.0001
ANOVA *P*†	0.16	0.49	0.39	0.90
Pair-wise comparisons	NS	NS	NS	NS

Data are the mean ± SD of epithelial defect in square millimeters.

* Paired *t*-test looking at the within-group change.

† ANOVA *P* for the overall differences between the three groups. If the ANOVA $P \leq 0.05$, then pair-wise comparisons were tested using multiple-comparison *t*-tests, which adjusts the α levels based on the number of pair-wise comparisons that were made.

Histologic Examination of Nontarget Organs

A major safety issue that had to be addressed in this study was the potential of an antiproliferative gene to cause corneal ulcers and necrosis of ocular adnexa or remote tissues. Histologic examination of paraformaldehyde-fixed sections of ocular adnexa (lower and upper eyelids), contralateral eyes, nasal mucosa, and nasal septa of dnG1 vector–treated rabbits showed no evidence of inflammation, ulceration, thrombosis, or hemorrhage in rabbits in which infectious keratitis did not develop. No pathologic abnormality was observed in tissue sections obtained from the brain, lung, heart, liver, spleen, kidney, testis, and ovary in dnG1 vector–treated rabbits, indicating absence of viral dissemination to nontarget organs.

Summary of Vector Toxicity and Biodistribution Studies

There was no morbidity or mortality associated with dnG1 vector ophthalmic treatment, and there was no convincing evidence of viral dissemination in nontarget organs of dnG1 vector–treated animals. Postoperative morbidity occurred in 2 (6%) of 30 rabbits, which was attributed to infection, because none of the rabbits received postoperative antibiotic treatment.

DISCUSSION

The use of photorefractive keratectomy (PRK) by excimer laser for correction of myopia, astigmatism, and hyperopia has gained increasing popularity in the ophthalmic community.[1,30] The 193-nm wavelength of the excimer radiation produces a photochemical reaction breaking the molecular bonds of collagen and other corneal components, leading to the ablation of tissue.[31,32] This mechanism of action allows the precise tissue removal of the anterior corneal surface with submicron accuracy, resulting in changes of the corneal curvature, and therefore, in the cornea's refractive power.[33] Similarly, PTK has been used as an effective method for the treatment of superficial corneal abnormalities.[34–37] However, the postoperative phenomenon of partial loss of corneal transparency, known as corneal haze, limits the success of both PRK and PTK. Lamellar keratectomy may be complicated by postoperative corneal opacification and loss of best corrected vision in approximately 10% of eyes.[5] Numerous studies indicate that corneal haze is mainly due to the uncontrolled proliferation of corneal keratocytes which produce extracellular matrix proteins and migrate to the anterior stromal compartment of the cornea.[2,38–40] Currently, there is no effective treatment to prevent these inappropriate wound-healing responses. Although mitomycin C has shown some success in favorably modulating the wound-healing process in rabbits,[41] experimental gene therapy emerges as another promising alternative.

TABLE 3. Mean Modified Draize Score for Ocular External Toxicity Assessment after Four Measurements

	Dose Level I	Dose Level II	Dose Level III
Mean Cumulated Score	2.0 ± 0.00	2.0 ± 0.53	2.65 ± 0.52

Five minutes after first vector eyedrop application and 5 minutes after last vector eyedrop application for 2 consecutive days (Mean ± SD). The highest possible score is 40.

In recent years, there has been a growing consensus that modulation of convergent pathways of cell activation and/or cell cycle control may lead to the development of more effective therapeutic strategies.[17,42,43] The present study extends the potential utility of gene therapy approaches directed against the cyclin G1 locus,[20] with the introduction of mutant cyclin G1 expression constructs designed to function in a dominant negative manner. Although the efficacy and the evaluation of antisense strategies are often problematic,[44–46] a mutant protein engineered to inhibit the function of its normal counterpart in a dominant fashion has the dual advantages of blocking the function of closely related (redundant) elements and of producing a detectable gene product (Fig. 1B). Retroviral vectors integrate randomly into the chromosome only in actively dividing cells, thus sparing normal nondividing cells. Cyclin G1 appears to be a survival factor for many proliferative cells, and the expression of the dnG1 protein in cells induces apoptosis and cell death. Therefore, the effect of dnG1 expression in cells is specific to proliferative cells, and the occurrence of long-term complications from persistent dnG1 production is not likely.

In the present study, we evaluated the efficacy and safety of eye drop applications of a mutant cyclin G1 retroviral vector as preventive treatment of laser-induced corneal haze in rabbits. The development of corneal haze 2 weeks after laser surgery was inhibited by eye drop applications of the dnG1 vector, and to a lesser extent, of the antisense cyclin G1 vector. Consistent with the slit lamp observations, inhibition of keratocyte proliferation and a dramatic reduction of abnormal extracellular

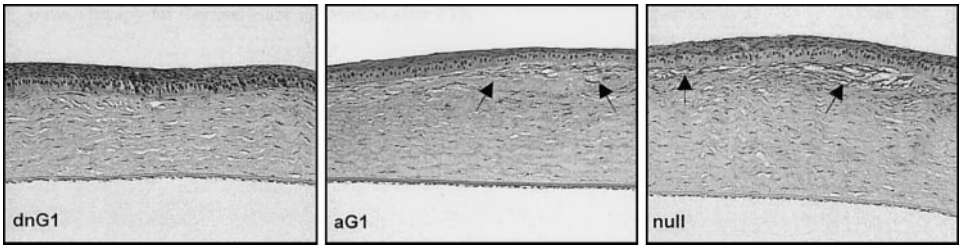

FIGURE 7. Keratocyte proliferation and subepithelial fibrosis in the aG1 (*middle*), and null (*right*) groups (*arrows*) but not in the dnG1 (*left*), corresponded well with the corneal haze scores previously obtained with the digital imaging system. No alterations of the cellular phenotype were observed in any of the studied groups.

matrix (i.e., intracellular fibronectin) production was noted in the dnG1 vector–treated corneas when compared with the null and aG1 vector–treated groups. Plausibly, the reduction in the severity of corneal haze can be attributed to the decreased number of proliferative keratocytes in the subepithelial compartment and consequently, reduced abnormal extracellular matrix deposition in the dnG1 vector–treated group.

Contrary to an expected delay in re-epithelialization with any antiproliferative agent applied to the corneal surface, the epithelial defect closure was not compromised by therapeutic doses of vector. Corneal ulcerations were not detected in any of the dnG1, aG1, or null vector-treated eyes. This may be accounted for by the basal and peripheral location of corneal epithelial stem cells and amplifying cells, which appear to be protected from vector exposure in the limbal area.[47,48] In addition, epithelial cells have shown poor transduction efficiency using retroviral agents in vivo.[1,49] Therefore, we believe that neighboring epithelial cells are not likely to be affected by the dnG1 retroviral vector, and because of the quiescent nature of corneal endothelial cells and their more distant location in relation to the area of vector application, it is unlikely that these cells would be similarly affected. Further, the modified Draize scores were similar among groups treated with increasing doses of the dnG1 vector, revealing minimal external ocular toxicity at vector doses planned for a human phase I clinical trial. Moreover, biodistribution studies showed no evidence of vector dissemination in neighboring and distant nontarget organs. The significance of the very-low-level PCR signals detected in the left lower eyelids of high-dose dnG1 vector–treated rabbits is uncertain. The absence of corneal ulceration and other histologic abnormalities in the treated eyes suggest that this finding may not be clinically significant. Finally, the apparent absence of necrosis, fibrosis, and deformation in dnG1 vector–treated corneas attests to the potential safety of this antiproliferative retroviral vector.

The characteristic exposure of extracellular matrix (ECM) components that promotes the adherence of vWF to vascular lesions has recently been exploited to therapeutic advantage

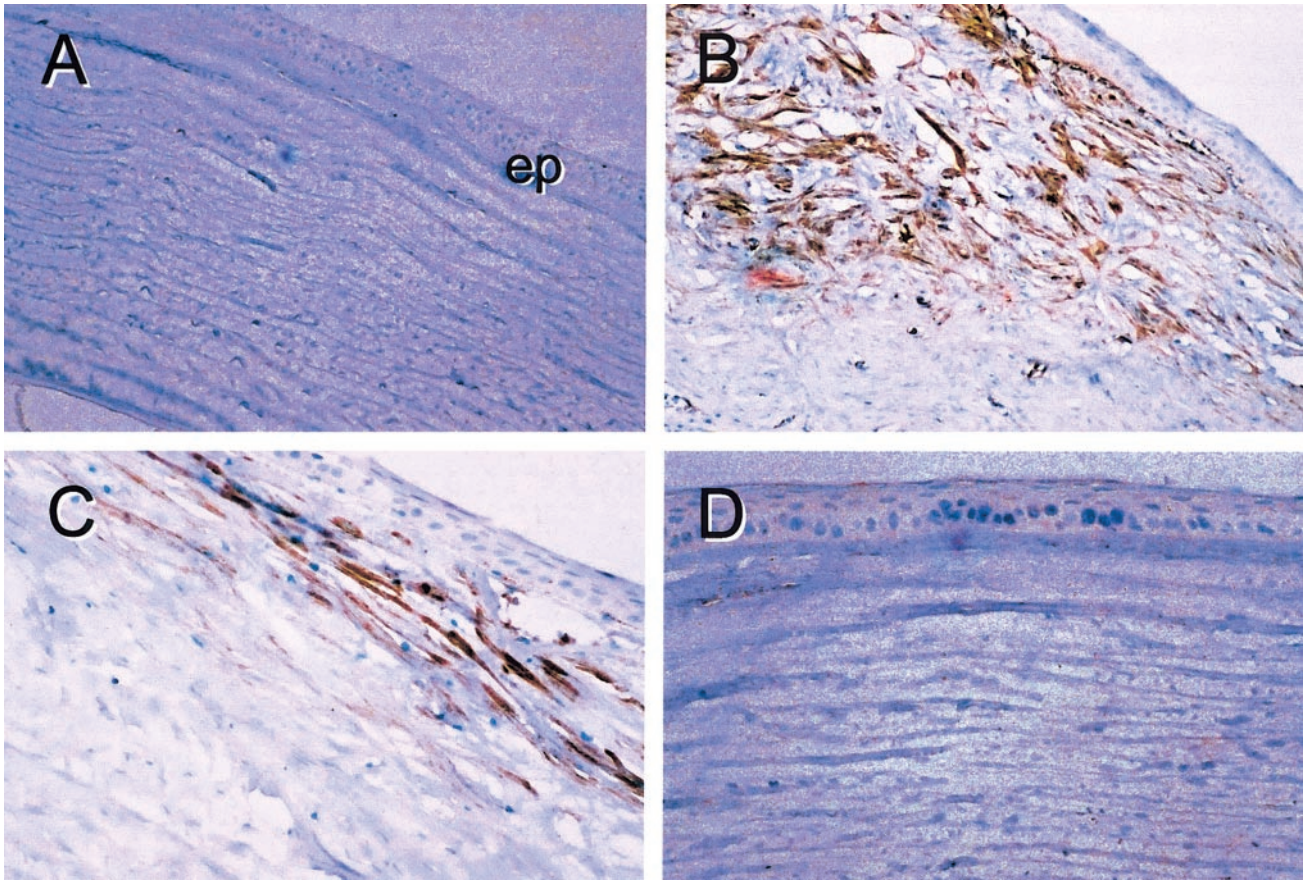

FIGURE 8. DRAMATIC REDUCTION OF EXTRACELLULAR MATRIX PROTEIN DEPOSITION IN DNG1 VECTOR–TREATED CORNEAS AFTER LASER TREATMENT. IMMUNOREACTIVE FIBRONECTIN STAINED *REDDISH-BROWN* IN THE SUBEPITHELIAL COMPARTMENT OF THE CORNEA. **(A)** NORMAL NONABLATED, **(B)** NULL VECTOR-TREATED, **(C)** AG1 VECTOR–TREATED, AND **(D)** DNG1 VECTOR–TREATED CORNEAS.

with the development of collagen-targeted retroviral vectors that concentrate viral particles at surgical sites and improve gene delivery to target cells.[23,27–29] This targeting strategy involves the genetic engineering of the Moloney murine leukemia (MLV) gp70 envelope (*env)* protein to display a collagen-binding decapeptide derived from the D2 domain of vWF (vWF-D2). The resultant vector exhibits a desired gain of function—that is, high binding affinity for collagen matrices—while retaining its ability to transfer genes into actively dividing cells. When injected intravenously, the collagen-targeted vector exhibits a lesion-seeking feature—that is, the ability to accumulate at sites of exposed collagen within cancerous or vascular lesions in the vicinity of target cells, enabling viral fusion and core entry through normal viral receptor pathways.[23,27–29] Among the virtues of this collagen-targeted retroviral vector system is that it enables a more efficient delivery of genes directly to surgical sites where collagen is exposed. For upcoming clinical trials, it incorporates features both of safety and efficacy. First of all, retroviral vectors have been used in at least 50% of gene therapy protocols and have an established track record of safety in more than 3000 patients. Second, improved retroviral vectors generated in human producer cells have been shown to be complement resistant,[50] with minimal immunogenicity,[29,51] which would enable multiple treatments. Third, the use of a transient transfection system for vector production, in which confluent producer cells are used, the packaging components are placed on separate plasmids,[18] and murine proviral sequences bearing little homology to human DNA sequences are used, reduces the risk of homologous recombination events that would generate a replication-competent retrovirus.[52] In addition, the use of a transient transfection system for retroviral vector production serves to ensure the fidelity of gene expression, particularly of antiproliferative constructs.[23] Finally, collagen-targeted vectors would facilitate preferential vector accumulation and integration at specific sites of laser surgery, thereby reducing the number of vector particles available for biodistribution to nontargeted organs,[29] and thus minimizing the incidence of systemic side effects.

We conclude that topical ophthalmic instillation of the dnG1 vector at the doses planned for a phase I clinical trial is potentially safe and effective in inhibiting the development of corneal haze after PTK. Taken together, these data support a rationale for the development of gene therapy protocols, using the collagen-targeted dnG1 retroviral vector for prevention of excimer laser–induced corneal haze.

References

1. Seiler T, McDonnell PJ. Excimer laser photorefractive keratectomy. *Surv Ophthalmol.* 1995;40:89–118.
2. Fantes FE, Hanna KD, Waring GO III, Pouliquen Y, Thompson KP, Savoldelli M. Wound healing after excimer laser keratomileusis (photorefractive keratectomy) in monkeys. *Arch Ophthalmol.* 1990;108:665–675.
3. Campos M, Raman S, Lee M, McDonnell PJ. Keratocyte loss after different methods of de-epithelialization. *Ophthalmology.* 1994; 101:890–894.
4. Szerenyi KD, Wang XW, Gabrielian K, McDonnell PJ. Keratocyte loss and repopulation of anterior corneal stroma after de-epithelialization. *Arch Ophthalmol.* 1994;112:973–977.
5. Wu WCS, Stark WJ, Green WJ. Corneal wound healing after 193 nm excimer laser keratectomy. *Arch Ophthalmol.* 1991;109:1426–1432.
6. Hanna KD, Pouliquen YM, Savoldelli M, et al. Corneal wound healing in monkeys 18 months after excimer laser photorefractive keratectomy. *Refract Corneal Surg.* 1990;6:340–345.
7. Tuft SJ, Zabel RW, Marshall J. Corneal repair following keratectomy: a comparison between conventional surgery and laser photoablation. *Invest Ophthalmol Vis Sci.* 1989;30:1769–1777.
8. Møller-Pedersen T, Li HF, Petroll WM, Cavanagh HD, Jester JV. Confocal microscopic characterization of wound repair after photorefractive keratectomy. *Invest Ophthalmol Vis Sci.* 1998;39: 487–501.
9. Jester JV, Petroll WM, Cavanagh HD. Corneal stromal wound healing in refractive surgery: the role of myofibroblasts. *Prog Retinal Eye Res.* 1999;18:311–356.
10. Møller-Pedersen T, Cavanagh HD, Petroll WM, Jester JV. Stromal wound healing explains refractive instability and haze development after photorefractive keratectomy. *Ophthalmology.* 2000; 107:1235–1245.
11. Kampmeier J, Behrens A, Wang Y, et al. Inhibition of rabbit keratocyte and human fetal lens epithelial cell proliferation by retrovirus-mediated transfer of antisense cyclin G1 and antisense MAT1 constructs. *Hum Gene Ther.* 2000;11:1–8.
12. Seitz B, Baktanian E, Gordon EM, Anderson WF, LaBree L, McDonnell PJ. Retroviral vector-mediated gene transfer into keratocytes: in vitro effects of polybrene and protamine sulfate. *Graefes Arch Clin Exp Ophthalmol.* 1998;236:602–612.
13. Seitz B, Moreira L, Baktanian E, et al. Retroviral vector-mediated gene transfer into keratocytes in vitro and in vivo. *Am J Ophthalmol.* 1998;126:630–639.
14. Pepose JS, Leib DA. Herpes simplex viral vectors for therapeutic gene delivery to ocular tissues. *Invest Ophthalmol Vis Sci.* 1994; 35:2662–2666.
15. Chang MW, Ohno T, Gordon D, et al. Adenovirus-mediated transfer of the herpes simplex virus thymidine kinase gene inhibits vascular smooth muscle cell proliferation and neointima formation following balloon angioplasty of the rat carotid artery. *Mol Med.* 1995;1:172–181.
16. Wu L, Liu L, Yee A, Carbonaro-Hall D, Tolo V, Hall F. Molecular cloning of the human CYCG1 gene encoding a G-type cyclin: overexpression in osteosarcoma cells. *Oncol Rep.* 1994;1:705–711.
17. Xu F, Prescott MF, Liu PX, et al. Long term inhibition of neointima formation in balloon-injured rat arteries by intraluminal instillation of a matrix-targeted retroviral vector bearing a cytocidal mutant cyclin G1 construct. *Int J Mol Med.* 2001;8:19–30.
18. Soneoka Y, Cannon PM, Ramsdale EE, et al. A transient three-plasmid expression system for the production of high titer retroviral vectors. *Nucleic Acids Res.* 1995;23:628–633.
19. Skotzko MJ, Wu LT, Anderson WF, Gordon EM, Hall FL. Retroviral vector-mediated gene transfer of antisense cyclin G1 (CYCG1) inhibits proliferation of human osteogenic sarcoma cells. *Cancer Res.* 1995;55:5493–5498.
20. Zhu NL, Wu L, Liu PX, et al. Down-regulation of cyclin G1 expression by retrovirus-mediated antisense gene transfer inhibits vascular smooth muscle cell proliferation and neointima formation. *Circulation.* 1997;96:628–635.
21. Chen DS, Zhu NL, Hung G, et al. Retroviral vector-mediated transfer of an antisense cyclin G1 construct inhibits osteosarcoma tumor growth in nude mice. *Hum Gene Ther.* 1997;8:1679–1686.
22. Hung G, Skotzko MJ, Chang M, et al. Intratumoral injection of an antisense cyclin G1 retroviral vector inhibits growth of undifferentiated carcinoma xenografts in nude mice. *Int J Pediatr Hematol Oncol.* 1997;4:317–325.
23. Gordon EM, Liu PX, Chen ZH, et al. Inhibition of metastatic tumor growth in nude mice by portal vein infusions of matrix-targeted retroviral vectors bearing a cytocidal cyclin G1 construct. *Cancer Res.* 2000;60:3343–3347.
24. Campos M, Cuevas K, Garbus J, Lee M, McDonnell PJ. Corneal wound healing after excimer laser ablation: effects of nitrogen gas blower. *Ophthalmology.* 1992;99:893–897.
25. Maldonado MJ, Arnau V, Martinez-Costa R, et al. Reproducibility of digital image analysis for measuring corneal haze after myopic photorefractive keratectomy. *Am J Ophthalmol.* 1997;123:31–41.
26. Imayasu M, Moriyama T, Ohashi J, Ichijima H, Cavanagh HD. A quantitative method for LDH, MDH and albumin levels in tears with ocular surface toxicity scored by Draize criteria in rabbit eyes. *CLAO J.* 1992;18:260–266.

27. Hall FL, Gordon EM, Wu L, et al. Targeting retroviral vectors to vascular lesions by genetic engineering of the MoMLV gp70 envelope protein. *Hum Gene Ther.* 1997;8:2183–2192.
28. Hall FL, Liu L, Zhu NL, et al. Molecular engineering of matrix-targeted retroviral vectors incorporating a surveillance function inherent in von Willebrand factor. *Hum Gene Ther.* 2000;11:983–993.
29. Gordon EM, Liu PX, Chen ZH, et al. Systemic administration of a matrix-targeted retroviral vector is efficacious for cancer gene therapy in mice. *Hum Gene Ther.* 2001;12:193–204.
30. McDonnell PJ. Emergence of refractive surgery. *Arch Ophthalmol.* 2000;118:1119–1120.
31. Pettit GH, Edinger MN, Weiblinger RP. Argon fluoride excimer laser ablation of cornea. *SPIE Proc.* 1992;1646:236–241.
32. Srinivasan R, Sutcliffe E. Dynamics of ultraviolet laser ablation of corneal tissue. *Ophthalmology.* 1987;103:470–471.
33. Munnerlyn CR, Koons SJ, Marshall J. Photorefractive keratectomy: a technique for laser refractive surgery. *J Cataract Refract Surg.* 1988;14:46–52.
34. Fong YC, Chuck RS, Stark WJ, McDonnell PJ. Phototherapeutic keratectomy for superficial corneal fibrosis after radial keratotomy. *J Cataract Refract Surg.* 2000;26:616–619.
35. Cavanaugh TB, Lind DM, Cutarelli PE, et al. Phototherapeutic keratectomy for recurrent erosion syndrome in anterior basement membrane dystrophy. *Ophthalmology.* 1999;106:971–976.
36. Orndahl MJ, Fagerholm PP. Treatment of corneal dystrophies with phototherapeutic keratectomy. *J Refract Surg.* 1998;14:129–135.
37. Dogru M, Katakami C, Miyashita M, et al. Visual and tear function improvement after superficial phototherapeutic keratectomy (PTK) for mid-stromal corneal scarring. *Eye.* 2000;14:779–784.
38. Fitzsimmons TD, Fagerholm P, Harfstrand A, Schenholm M. Hyaluronic acid in the rabbit cornea after excimer laser superficial keratectomy. *Invest Ophthalmol Vis Sci.* 1992;33:3011–3016.
39. Gaster RN, Binder PS, Coalwell K, Berns M, McCord RC, Burstein NL. Corneal surface ablation by 193 nm excimer laser and wound healing in rabbits. *Invest Ophthalmol Vis Sci.* 1989;30:90–98.
40. Wilson SE. Molecular cell biology for the refractive corneal surgeon: programmed cell death and wound healing. *J Refract Surg.* 1997;13:171–175.
41. Jain S, McCally RL, Connolly PJ, Azar DT. Mitomycin C reduces corneal light scattering after excimer keratectomy. *Cornea.* 2001; 20:45–49.
42. Pellegrini G, Golisano O, Paterna P, et al. Location and clonal analysis of stem cells and their differentiated progeny in the human ocular surface. *J Cell Biol.* 1999;145:769–782.
43. Kruse FE, Volcker HE. Stem cells, wound healing, growth factors, and angiogenesis in the cornea. *Curr Opin Ophthalmol.* 1997;8: 46–54.
44. Couderc BC, de Neuville S, Douin-Echinard V, et al. Retrovirus-mediated transfer of a suicide gene into lens epithelial cells in vitro and in an experimental model of posterior capsule opacification. *Curr Eye Res.* 1999;19:472–482.
45. Andres V. Control of vascular smooth muscle cell growth and its implication in atherosclerosis and restenosis (review). *Int J Mol Med.* 1998;2:81–89.
46. Braun-Dullaeus RC, Mann MJ, Dzau VJ. Cell cycle progression: new therapeutic target for vascular proliferative disease. *Circulation.* 1998;98:82–89.
47. Morishita R, Gibbons GH, Horiuchi M, et al. A gene therapy strategy using a transcription factor decoy of the E2F binding site inhibits smooth muscle proliferation in vivo. *Proc Natl Acad Sci USA.* 1995;92:5855–5859.
48. Simons M, Edelman ER, DeKeyser JL, Langer R, Rosenberg RD. Antisense c-myb oligonucleotides inhibit intimal arterial smooth muscle cell accumulation in vivo. *Nature.* 1992;359:67–70.
49. Shi Y, Fard A, Galeo A, et al. Transcatheter delivery of c-myc antisense oligomers reduces neointima formation in a porcine model of coronary artery balloon injury. *Circulation.* 1994;90: 944–951.
50. Pensiero MN, Wysocki CA, Nader K, Kikuchi GE. Development of amphotropic retrovirus vectors resistant to inactivation by human serum. *Hum Gene Ther.* 1996;8:1095–1101.
51. Fong TC, Sauter SL, Ibanez CE, Sheridan PL, Jolly DJ. The use and development of retroviral vectors to deliver cytokine genes for cancer therapy. *Crit Rev Ther Drug Carrier Systems.* 2000;17:1–60.
52. Markowitz D, Goff S, Banks A. Construction and use of a safe and efficient amphotropic packaging cell line. *Virology.* 1988;167: 407–414.